Source: *SPIE 11th Annual International Symposium on Smart Structures and Materials*, San Diego, CA, USA, March 14-18, 2004

Design of a Wireless Active Sensing Unit for Structural Health Monitoring

Jerome P. Lynch*[a], Arvind Sundararajan[b], Kincho H. Law[b], Hoon Sohn[c] and Charles R. Farrar[c]
[a]Dept. of Civil and Environmental Engineering, University of Michigan, Ann Arbor, MI 48109
[b]Dept. of Civil and Environmental Engineering, Stanford University, Stanford, CA 94305
[c]Engineering Sciences and Applications, Los Alamos National Laboratory, Los Alamos, NM 87545

ABSTRACT

Many academic and commercial researchers are exploring the design and deployment of wireless sensors that can be used for structural monitoring. The concept of intelligent wireless sensors can be further extended to include actuation capabilities. In this study, the design of a wireless sensing unit that has the capability to command active sensors and actuators is proposed for structural monitoring applications. Active sensors are sensors that can input excitations into a structural system and simultaneously monitor the corresponding system's response. The computational core of the wireless active sensing unit is capable of interrogating response data in real time and can be used to execute embedded damage detection analyses. With high-order vibration modes of structural elements exhibiting greater sensitivity to damage than global structural modes, wireless active sensors can play a major role in a structural health monitoring system because they are capable of exciting high-order modes. A computational framework for analyzing piezoelectric based active sensor signals for indications of structural damage is proposed. For illustration, a simple aluminum plate with piezoelectric active sensors mounted to its surface is used.

Keywords: Wireless active sensors, structural health monitoring, sensing networks, active sensors

1. INTRODUCTION

The poor state of our national infrastructure underscores the need for low-cost structural monitoring systems that can track the performance of structures over their entire operational lives. Data collected by permanently installed monitoring systems can offer opportunities to rapidly assess the condition of a structure's overall integrity and allow structural damage to be repaired when it occurs. Response measurements could also provide a better understanding of structural live loads and structural nonlinear behavior under seismic loadings. In response to these needs, many have begun to experiment with new technologies such as wireless communications, microelectromechanical system (MEMS) sensors and mobile computing to improve current structural monitoring practices. For example, researchers are exploring the adoption of wireless radios for communication of measurement data in structural monitoring systems in order to reduce the high costs associated with the installation of wires between sensors and centralized data repositories[1]. Lynch *et al.*[2] have extended this work to include embedded microcontrollers within a wireless sensing unit prototype; embedded microcontrollers can be loaded with numerical algorithms to locally process and interrogate measurement data directly at the sensor. This convergence of wireless communications, embedded computing and sensors is creating exciting opportunities to improve the functional features of current wire-based monitoring systems, while simultaneously reducing their costs. The advantages of a wireless structural monitoring system have recently been illustrated during forced vibration testing of the Alamosa Canyon Bridge in southern New Mexico. During testing, the bridge was instrumented with wireless sensing units and MEMS accelerometers to monitor the bridge's response to modal hammer blows and traffic loads. To benchmark the performance of the wireless monitoring system, a commercial wire-based (tethered) monitoring system was installed in parallel. The vibration tests conducted on the Alamosa Canyon Bridge have revealed a number of important findings[3]: 1) wireless sensing prototypes were capable of collecting sensor data with high precision, 2) bridge modal frequencies were accurately determined using a fast Fourier transform (FFT) embedded in and executed by the wireless sensing unit core, and 3) the installation of the wireless monitoring system was completed in approximately half the time required by the tethered wire-based system.

*jerlynch@umich.edu; phone 1-734-615-5290; fax 1-734-764-4292; http://www-personal.engin.umich.edu/~jerlynch/

With embedded computing coupled with the sensor, algorithms that automate the interrogation of response data can be executed in real-time. One set of algorithms being considered for inclusion in a wireless sensor is one that would interrogate data for indications of structural damage. A majority of the damage detection methods previously considered for civil structures depend on changes in the global vibration characteristics of structural systems for the identification of the existence, location and severity of damage[4]. The cost of wire-based monitoring systems tends to limit the number of sensors that can be economically installed in a structure. Global vibration characteristics offer an attractive alternative because they can identify damage using the small number of sensors available without having to be collocated in the vicinity of the damage. Unfortunately, the complexities of civil structures pose unique challenges that often render global vibration-based damage detection ineffective[5]. First, accurate measurements of global modal properties are difficult to obtain using experimental response data. In addition, subtle changes in modal properties are often masked by changes originating from environmental influences such as temperature and humidity. Finally, low-order modes (defined at low frequencies) are known to be less sensitive to subtle levels of structural damage.

As the cost of wireless monitoring systems continue to decline, sensor networks defined by high nodal densities are now possible. Structural monitoring systems with a large number of sensor nodes can measure the global response of the structure in addition to the behavior of individual structural elements. With high-order modal vibration characteristics of structural elements more reliable for damage detection, monitoring key structural elements can represent an attractive and effective monitoring strategy[6]. In addition, damage detection algorithms focused on local responses of the structure (e.g., vibrations in a beam) would not require the transfer of data from many wireless sensors thereby preserving the autonomy of the computationally self-sufficient wireless sensing unit. Otherwise, response time-histories of the global system would need to be wirelessly communicated between sensor nodes resulting in rapid depletion of portable power sources, such as batteries.

In recent years, a new sensing paradigm, termed active sensing, has emerged and has been shown to be an effective tool for structural health monitoring. The vast majority of sensors used in structural engineering are passive since they only measure structural responses to external loads, which they have no control over. In contrast, an active sensor can excite a structural system and record the structural response that it has initiated[7]. An attractive feature of active sensors lies in the fact that their excitations can be precisely repeated. In recent years, active sensing has grown in popularity and has begun to be explored for detection of damage in civil structural systems; active sensors often excite a structure in a local area with low energy excitations. With many structural elements (e.g. beams, columns, truss elements, joints) exhibiting sensitivity to damage at high-order modal frequencies, active sensors can conveniently excite structural elements using high frequency banded excitations. To date, the majority of active sensors investigated have been based on the use of piezoelectric materials to excite and sense the structural system. Park *et al.*[6] have illustrated the utility of measuring the electrical impedance of piezoelectric elements mechanically coupled to a structure's surface. Termed the electro-mechanical impedance (EMI) method, damage in the vicinity of the piezoelectric element causes noticeable change in the real component of the complex impedance of the coupled piezoelectric-structural system. Their approach has been shown to successfully detect the onset of cracking in masonry structures and bolt loosening in steel truss joints. Bhalla and Soh[8] find similar results when the EMI method was applied to a reinforced concrete frame system. In another technique, Wu and Chang[9] have employed piezoelectric rings mounted to steel reinforcement bars encased in concrete elements to accurately detect debonding damage. Their findings reveal debonding of the reinforcement element causes an increase in the amplitude envelopes of high-frequency sinusoidal signals transmitted across the steel bar from one piezoelectric pad to another. All of these methods employ excitation signals defined by high frequency content well above 1 kHz. While high frequency signals are effective in exciting the high-order modes of structural elements, they quickly attenuate in structural materials. As a result of the spatial attenuation of the active sensor excitation, damage detection performed using active sensors often focuses on localized areas near the active sensor.

This paper describes the architectural design of a wireless active sensing unit that can improve the functionality of structural health monitoring systems. In particular, wireless sensors are enhanced with the ability to apply actuation forces into the structure. The wireless active sensing unit's high-speed actuation interface is designed to facilitate the use of all types of active sensors and structural actuators in a monitoring system. So that the high-order modes of structural elements can be illuminated, the actuation and sensing interfaces are both designed to have high sampling rates of 40 kHz. After completion of the wireless active sensing unit, embedded software is written to operate the unit and to interrogate measurement data. To showcase the capabilities of the unit's computational core, a software framework that

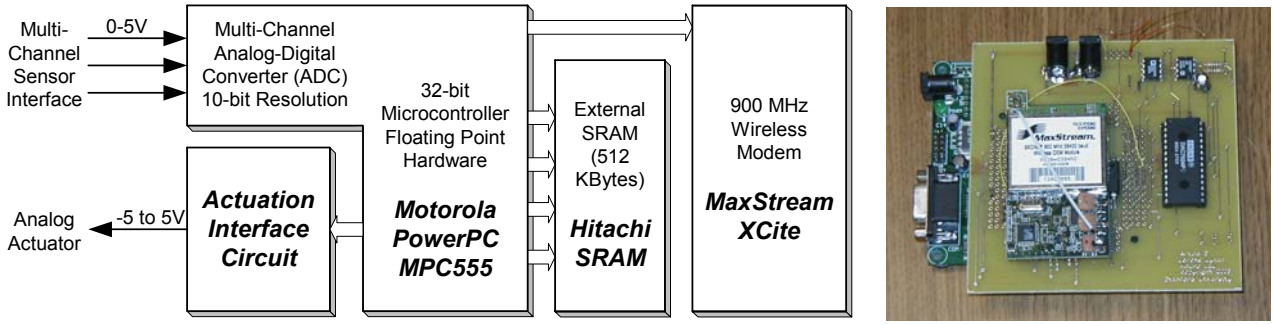

Fig. 1 Architectural design of the wireless active sensing unit

supports the autonomous execution of damage detection analyses is presented. An aluminum plate actively sensed by piezoelectric pads is employed to illustrate the performance of the wireless active sensing unit's hardware and software.

2. DESIGN OF A MULTI-FUNCTIONAL WIRELESS ACTIVE SENSING UNIT

To monitor the health of key elements within civil structures, the design of a wireless active sensing unit based on low-cost off-the-shelf components is proposed. The architectural design of the unit can be divided into four functional subsystems (sensor interface, actuation interface, computational core and wireless communication channel) whose interoperability is described by Fig. 1. The computational core is the most important element of the unit design since it will be responsible for the overall operation of the unit, will control the actuation, sensing and wireless interfaces and must execute embedded algorithms that interrogate measurement data.

2.1 PowerPC-Based Computational Core

The computational core is designed to support the autonomous operation of the wireless active sensing unit. Some of the key roles the computational core will play include operation of sensing and actuation interfaces, management of measurement data, execution of embedded analysis procedures and control of the flow of information through the wireless modem. With embedded system microcontrollers well suited to address the tasks of the computational core, the Motorola PowerPC MPC555 microcontroller, with an internal 32-bit architecture, is chosen for the design of the wireless active sensing unit[10]. The Motorola MPC555 operates at clock frequencies as high as 40 MHz and internally integrates a floating-point arithmetic unit for single-cycle floating point calculations. The high speed of the processor will be especially useful if active sensors with high frequency operational ranges are connected to the unit. Coupled with this fast processor is 448 Kbytes of internal read-only memory (ROM) where firmware will be stored for unit operation and execution of embedded data processing algorithms. The MPC555 also has 26 Kbytes of internal random access memory (RAM) that could be used to store temporary data generated by executing programs running from ROM. Since the size of the internal RAM bank is too small for storing sensor measurements, an external static RAM (SRAM) integrated circuit (IC) is added to the unit design to provide additional memory for data storage. The current prototype uses the Hitachi HM628512B SRAM IC, providing 512 Kbytes of memory storage

2.2 Sensing Interface for Analog Sensors

For digitization of measurement data from structural sensors, the MPC555 internal analog-to-digital converter (ADC) will be employed. The 10-bit ADC can accommodate 32 simultaneous sensing channels with sampling rates as high as 100 kHz. Additional conversion resolutions can be gained by employing over sampling techniques or through the use of low-noise amplification circuits. To manage the sensing interface in real-time, the MPC555 interrupt service routines are utilized to ensure data is read on a strict timing schedule. Unfortunately, inherent latencies incurred by servicing the interrupts reduce the maximum ADC sampling rate to speeds of 40 kHz.

2.3 Actuation Interface for Active Sensors and Structural Actuators

An actuation interface is responsible for providing command signals to a broad range of active sensors or actuators installed within a structural system. A digital-to-analog converter (DAC) that converts digital command signals

generated by the MPC555 into analog representations acceptable for commanding the actuators is at the core of the actuation interface. The Texas Instruments DAC7624 accepts 12-bit digital samples in parallel and outputs a zero-order-hold (ZOH) analog signal from 0 to 2.5 V on four selectable channels[11]. Using only one channel of the DAC, the settling time associated with each conversion is 10 μsec (100 kHz sampling rate). To improve the voltage range of the DAC, the DAC output signal is connected to the input of an instrumentation amplifier that can range shift and amplify the signal. An Analog Devices AD620 amplifier is chosen to shift the DAC output to a zero mean (from 1.25 V) and to amplify the signal by 4. This results in a completed actuation interface capable of outputting command voltages from -5 to +5 V. Similar to the sensing interface, embedded firmware written to service the actuation interface in real-time will reduce the speed of the actuation interface to 40 kHz.

2.4 Spread Spectrum Wireless Communications

The use of wireless communications will immediately alleviate some of the burdens of installing and maintaining cables in a structure. However, to be an effective substitute for cables, wireless radios chosen for integration with the wireless active sensing unit must be low-cost, far reaching and highly reliable. Previous wireless sensing unit designs have employed wireless modems such as the Proxim ProxLink and Proxim RangeLAN2 radio modems[2]. While both Proxim radios can propagate over 300 m in unobstructed open space, they consume over 150 mA of electrical current when transmitting and receiving data. To improve the power consumption characteristics of the wireless active sensing unit, a new wireless radio is considered for integration; in particular, the MaxStream XCite radio is chosen. The XCite communicates on the unregulated 900 MHz radio band and can communicate with over-the-air data rates of 38,400 bits per second. The open space communication range of the radio is 300 m but is only approximately 90 m when used in the interior of structures[12]. In contrast to the Proxim modems, the XCite radio only consumes 55 mA when transmitting data and 35 mA when receiving data. Use of the XCite radios reduce by at least one third the power consumption demands of the Proxim radios without sacrificing the distance the radios can communicate. When the radios utilize the wireless channel, frequency hopping spread spectrum encoding is employed ensuring the radio channel is highly reliable and resilient to narrow-band interference.

2.4 Prototype Fabrication

To construct a final prototype, a stacked circuit board approach is taken to the construction of the wireless active sensing unit. Board stacking will allow the unit form factor to be minimized and will make future upgrades to the hardware easier to complete. First, the Motorola MPC555 is purchased as a small starter development kit from Axiom (PB-555) where the microcontroller is mounted on a small-footprint (9 cm by 9 cm) printed circuit board (PCB). The output pins of the MPC555 are provided as header rows on the development kit board. The header rows of the Axiom board will be conveniently used to mount custom made printed circuit boards on top. To house the actuation interface circuit and the external SRAM IC, a PCB is designed and fabricated. This circuit board has the same dimensions as the MPC circuit board. The MaxStream wireless radios are purchased from the manufacturer on their own circuit board (4 cm by 7 cm) and are placed as a third layer over the actuation interface circuit board. Shown in Fig. 2 is the completed printed circuit board stack (3 circuit boards) assembled as a single wireless active sensing unit. The final dimensions of the fully assembled wireless active sensing unit are 9 cm by 9 cm in area and 4 cm in height. The cost of constructing the prototype, including the cost of the wireless modem, is approximately $250. However, the cost and form factor can both be substantially reduced if the wireless active sensing unit is commercially manufactured.

2.5 Power Sources and Anticipated Operational Life

In realistic field deployments, batteries are a likely power source for the wireless active sensing unit. Wireless active sensing units embedded in infrastructure systems can often be in difficult to reach locations making battery replacement a daunting task. The power demands of wireless sensors and the associated life expectancies of battery packs are important constraints to consider in the design of the final unit. Previous wireless sensing unit designs have selected low-power integrated circuit elements to minimize the overall power demand of the assembled unit. Local data interrogation at the wireless sensor has also been identified as a mechanism by which considerable battery power can be preserved[13]. The wireless active sensing unit proposed in this study does not minimize the total power consumption demand because attainment of a high-frequency actuation interface presented sufficient technical challenges. However, future iterations on the design of the wireless active sensing would attempt to minimize power consumption through the selection of low-power components or through the design of a two microcontroller computational core[2].

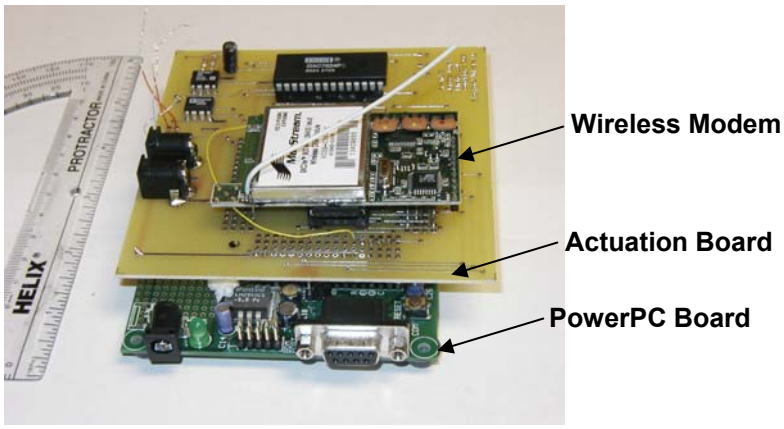

Fig. 2. Three printed circuit board stack assembled as a single wireless active sensing unit prototype

Table 1. Operation Power Schedule of the Prototype Wireless Active Sensor

Unit Component	Reference Voltage (V)	Electrical Current (mA)	Operational Power (mW)
Microprocessor			
MPC555 PowerPC	3.3	110	363
Actuation Interface:			
DAC Converter	5	3	15
Amplifier	9	5	45
Piezoelectric Actuators	-5 to 5	0 to 5	0 to 25
Wireless Modem:			
MaxStream XCite Radio	5	55	275

To assess the total amount of power required by the fully assembled wireless active sensing unit prototype, electrical currents are measured throughout the circuit. Table 1 summarizes the measured electrical currents and the respective power consumed. To serve as an example of a typical active sensor that could be interfaced to the unit, the power required to command a piezoelectric actuator is measured. The power expended in operating a piezoelectric element is a function of the command voltage applied. Considering the maximum command (+5 V) that can be given to a piezoelectric element by the unit, the worse case power consumption of the actuator is determined to be 25 mW. Based on the current draw of the unit's electrical components, if a lithium battery pack with high energy density is considered as a portable power source, a continuous operational life span of approximately 20 hours is expected[14]. Using a separate battery pack, approximately 28 hours of continuous battery life can be expected for the wireless modem. In the field, duty cycle usage of the wireless active sensing units can extend the life expectancy of the battery packs. For example, if a 0.1% duty usage cycle is employed (i.e. 90 seconds of usage every day), the anticipated life expectancy of the battery packs is on the order of 2 years.

3. PERFORMANCE VALIDATION OF A WIRELESS ACTIVE SENSING UNIT

To validate the performance of the fabricated wireless active sensing unit design, a 0.3175 cm thick aluminum plate, roughly 28.6 cm long and 6.8 cm wide, will be used. Mounted to the surface of the same side of the aluminum plate are two 1.43 cm square piezoelectric pads separated by 18.9 cm. One pad is to be used as an actuator for the emission of acoustic surface waves along the bar's length. The second pad will be used as a sensor to measure the acoustic waves received. A picture of the aluminum plate and mounted piezoelectric pads is presented in Fig. 3. The two piezoelectric

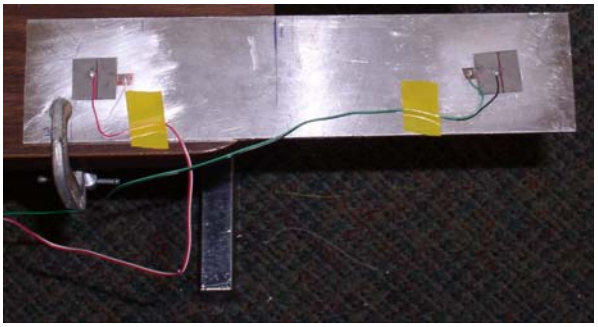

Fig. 3. Cantilevered aluminum bar with piezoelectric pads mounted to the top surface

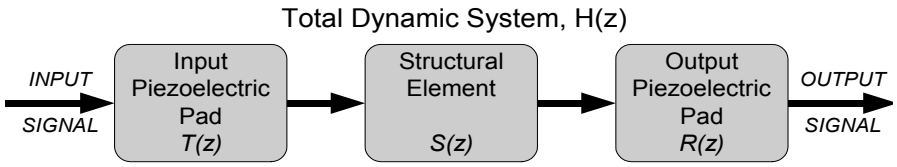

Fig. 4. Segmentation of the experimental aluminum bar setup into distinct dynamic subsystems

pads will be simultaneously actuated and sensed using a single wireless active sensing unit. In effect, the wireless active sensing unit closes an active sensing feedback loop between the two piezoelectric pads. The bar is cantilevered 22.57 cm over the edge of a table surface to which one end of the aluminum bar is clamped. The transmitting pad will remain on the side of the table while the receiving pad will be on the cantilevered end of the bar.

A series of excitations, as commanded by the wireless active sensing unit core, are emitted by the transmitting piezoelectric pad into the aluminum element. The acoustic wave produced transverses the bar's length and is observed by the receiving piezoelectric pad. Employing two piezoelectric elements on a single structural element aims at obtaining the complete input-output behavior of the structural element system. Driving the actuation and sensing interfaces at their maximum speeds of 40 kHz, the response modes of the aluminum plate below the Nyquist frequency (20 kHz) will be illuminated by the input excitations applied to the system. In the aluminum plate setup, the total dynamic system can be segmented into three dynamic elements: the two piezoelectric pads and the aluminum bar as shown in Fig. 4. Assuming each element to be linear and time invariant (LTI), each can be characterized by linear transfer functions in both the continuous and discrete-time complex domains (*s*- and *z*-domains respectively). In the discrete-time domain, the transfer function of the input piezoelectric, structural element and output piezoelectric are denoted as *T(z), S(z)* and *R(z)*, respectively. The total dynamic system transfer function, *H(z)*, can be characterized from the input voltage signal applied to the transmitting piezoelectric pad and the output signal from the receiving pad. In the complex *z*-domain, the discrete-time convolution sum is simply the multiplication of the individual transfer functions:

$$H(z) = T(z)S(z)R(z) \tag{1}$$

To characterize the transfer function describing the input-output behavior of the aluminum plate, a white noise input signal is applied by the transmitting piezoelectric pad. White noise is a convenient excitation source because its power spectral density is constant across the frequency band of interest and will excite all of the element vibration modes below the Nyquist frequency (20 kHz). To accurately determine the vibration characteristics of the aluminum plate, the presence of small levels of electrical and thermal noise in the sensing and actuation interfaces must be accounted for. Difficult to theoretically model, the noise can be accounted for by applying a large set of excitation sources. System parameters (e.g. modal frequencies) calculated from the input-output system signals can then be averaged across the signal sampling set to eliminate variability due to noise. In total, twenty white noise input excitations are applied to the aluminum plate with varying levels of signal energy. All of the white noise signals are chosen to have zero mean but

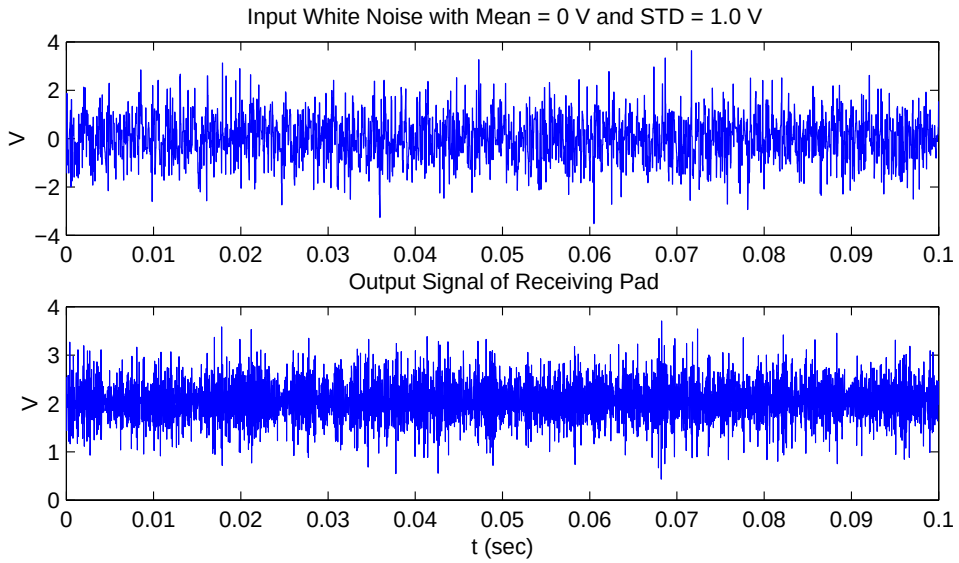

Fig. 5. (Top) white noise excitation with a 1.0 V standard deviation; (bottom) measured response of the aluminum plate

their standard deviation are varied between 0.3 V to 1.2 V. The response of the aluminum plate, as measured by the second piezoelectric pad, to an input white noise excitation with a 1.0 V standard deviation is shown in Fig. 5.

4. EMBEDDED SOFTWARE FOR LOCAL DAMAGE DETECTION

With ample amounts of memory and computational power integrated in the wireless active sensing unit design, input-output time history data of an actively sensed structural element can be analyzed in near real-time for the detection of damage. A novel damage detection methodology recently proposed by Lynch[15] to monitor the health of structural elements that are excited by active sensors is considered for inclusion in the core of the wireless active sensing unit. The damage detection methodology is capable of detecting damage using the location of system identification model poles. As damage is incurred in the structural element, subsequent changes in the frequency and damping ratio of high-order vibration modes will cause a migration of the transfer function poles (roots) in the discrete-time complex plane. Using the poles as features, linear classification boundaries are calculated that attempt to separate the poles of an unknown (damaged or undamaged) structural state from those of the undamaged structure. The quality of the decision boundary, as measured by the number of misclassifications, provides a measure of the statistical separability of transfer function poles that correspond to the unknown and undamaged structural element; pole clusters separable indicate the structural element is damaged. This method has been shown to be a powerful tool for detecting the presence of structural damage as well as providing an estimate of its severity in elements actively sensed using piezoelectric pads. With transfer function poles serving as the key feature of the method, the poles are determined from an auto-regressive with exogenous inputs (ARX) time-series model calculated using the input-output behavior of the structural element. Fig. 6 summarizes the steps taken by the computational core in autonomously executing this novel damage detection procedure. The steps corresponding to the ARX model will be described in more detail.

3.1 Embedment of ARX Time-Series Models

Software is written for the PowerPC microcontroller that will calculate an ARX time-series model based on the input-output response of the actively sensed aluminum plate element. Many numerical methods are available for determination of an ARX time series model, but least-squares estimation has been selected in this study. Defining the input to the system at the discrete time-step k by the variable $u(k)$, and the output, $y(k)$, an ARX time-series model can be written[16]:

$$y(k) + a_1 y(k-1) + \cdots a_{n_a} y(k-n_a) = b_1 u(k-1) + \cdots b_{n_b} u(k-n_b) + e(k) \tag{2}$$

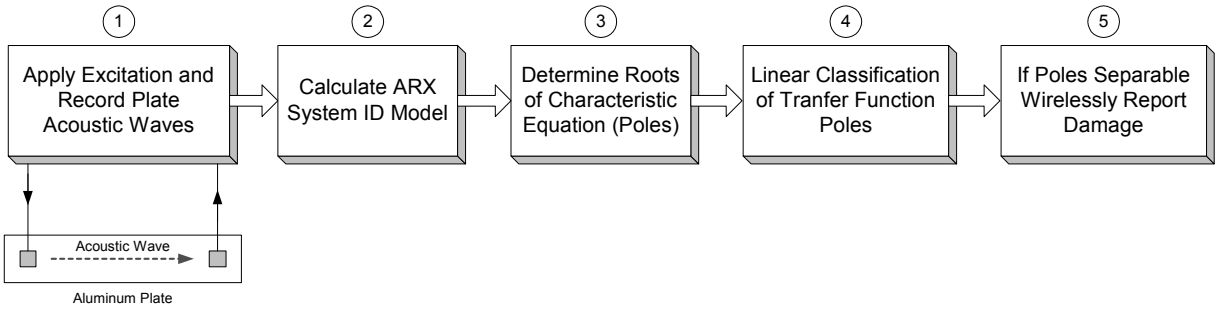

Fig. 6. Embedded damage detection methodology based on the migration of transfer function pole locations

where weights on observations of the system output and input are denoted as a and b, respectively. In total, n_a coefficients are applied to the outputs while n_b coefficients are applied to past inputs of the dynamic system. In this study, the system input, u, corresponds to the voltage applied to the first piezoelectric pad while the output, y, is the voltage measured from the second piezoelectric pad. In most cases, the ARX time-series model calculated will not precisely fit the measurement data resulting in a model error denoted as $e(k)$. To calculate the coefficients of the ARX model, a least squares estimation approach is taken to find the optimal ARX coefficients that minimize a quadratic cost function of the model error time-history vector, e:

$$J = \frac{1}{2} e^T e \tag{3}$$

With Equation (2) holding true for all observations of $y(k)$ from $k = n_a$ to N, a matrix representation of the ARX model, A, relating a vector of the coefficients of the model, c, to the time-history output, y, can be assembled:

$$y = \begin{Bmatrix} y(n_a+1) \\ y(n_a+2) \\ \vdots \\ y(N) \end{Bmatrix} = \begin{bmatrix} y(n_a) & \cdots & y(1) & u(n_a) & \cdots & u(n_a-n_b+1) \\ y(n_a+1) & \cdots & y(2) & u(n_a+1) & \cdots & u(n_a-n_b+2) \\ \vdots & \ddots & \vdots & \vdots & \ddots & \vdots \\ y(N-1) & \cdots & y(N-n_a) & u(N-1) & \cdots & u(N-n_b) \end{bmatrix} \begin{Bmatrix} -a_1 \\ \vdots \\ -a_{n_a} \\ b_1 \\ \vdots \\ b_{n_b} \end{Bmatrix} = Ac \tag{4}$$

To accurately determine the coefficients of an ARX model, many more response samples are collected than the number of coefficients ($N >> n_b + n_a$). In this case the measurement matrix, A, will be over-determined and full rank. To find the ARX model coefficients, the least-square solution of Equation (4) is given by:

$$c = \left(A^T A\right)^{-1} A^T y \tag{5}$$

Subroutines for embedment in the wireless sensing unit core are written in C, a high-level programming language. These subroutines are intended to calculate the least square solution to Equation (4). Singular value decomposition is employed in the solution to ensure its accuracy while a recursive batch algorithm for the final solution is taken to preserve space in memory[17].

3.2 ARX Model Size Selection

To accurately model the input-output response time-histories using an ARX model, the size of the ARX model needs to be chosen *a priori*. Size refers to the number of coefficients required to minimize the prediction error of the model. When fitting ARX models to system response data, the size of the model will dictate its predictive qualities. Generally, as sizes grow, model prediction errors will reduce. However, models too large are not necessarily better because they will over fit the measurement data; over fitting refers to the model capturing the behavior of signal noise in addition to the system's physical behavior. To assist in selecting a suitable ARX model size that only characterizes structural behavior, two pairs of input-output time-history records are needed: the first is designated for calculation of the model and the second to verify the model prediction error. Using the first pair of input-output data, ARX model coefficients are

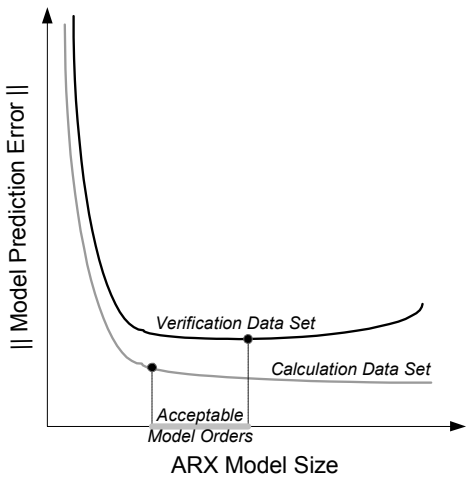

Fig. 7. Behavior of the ARX prediction error for the calculation and verification data set as model order increase

calculated for various model sizes. Once the model is determined, its predictive error is calculated using the training as well as the validation data sets. The vector norm of the model's prediction error is a reasonable scalar quantity that can be used to quantify the model's quality with smaller norms indicating a better fit to the input-output data. At first, when the model size begins to increase, the norm of the prediction error of the ARX model using both sets of input-output data will rapidly decrease. This indicates the larger models are capturing the structural system's dynamics more completely. As the model size continues to grow, improvements in the model prediction error will occur at an increasingly slower rate. At one point, larger models will start to include signal noise; at this point, the prediction error of the second verification data set will begin to increase. Fig. 7 summarizes the anticipated behavior of the ARX prediction error as a function of the model size. The final model size chosen should be sufficiently large to completely characterize the system without including signal noises in the model. For example, an acceptable ARX model size could be chosen from the region delineated in Fig. 7.

To determine the ideal ARX model size for the aluminum plate element, the 0.3V input signal and corresponding output response are chosen as the first data set to which ARX models of various sizes will be fit. As the verification set, the input-output response data from the 0.4V input signal is chosen. The selection of these two input-output data sets was arbitrary. Fig. 8 plots the ARX model prediction error for various model sizes. In each of the six plots in Fig. 8, one model order (either n_a or n_b) is held constant while the other is varied. Considering the prediction error of the ARX model as a function of n_a (n_b held fixed), we find the norm of the error decreases as expected. However, increases in the prediction error for the validation data set do not occur until large model orders in excess of $n_a = 100$ are considered. With only minor reduction in the model prediction error after $n_a = 21$ and the computational demand of calculating the ARX coefficients increasing, the ARX model order, $n_a = 21$, is chosen. Considering the prediction error as a function of n_b, the error norm corresponding to the validation data set increases after a model order of $n_b = 4$. As a result, the final ARX model order is chosen to be $n_a = 21$ and $n_b = 4$ and is denoted as ARX(21,4).

3.3 ARX Model Transfer Function Poles

After the ARX time-series model has been found for a set of input-output time-histories, the discrete-time transfer function of the system can easily be derived. The *Z*-transform is employed to transfer the discrete-time time-series described by Equation (2) into the complex *z*-domain:

$$\begin{aligned} Z\{y(k)+a_1y(k-1)+\cdots a_{n_a}y(k-n_a)=b_1u(k-1)+\cdots b_{n_b}u(k-n_b)+e(k)\}\Rightarrow \\ Y(z)+a_1z^{-1}Y(z)+\cdots a_{n_a}z^{-n_a}Y(z)=b_1z^{-1}U(z)+\cdots b_{n_{ba}}z^{-n_b}U(z)+E(z) \end{aligned} \tag{6}$$

If the residual error, *e(k)*, of the ARX time-series model is ignored, the transfer function of the dynamic linear system can be written in the discrete-time complex domain, *H(z)*:

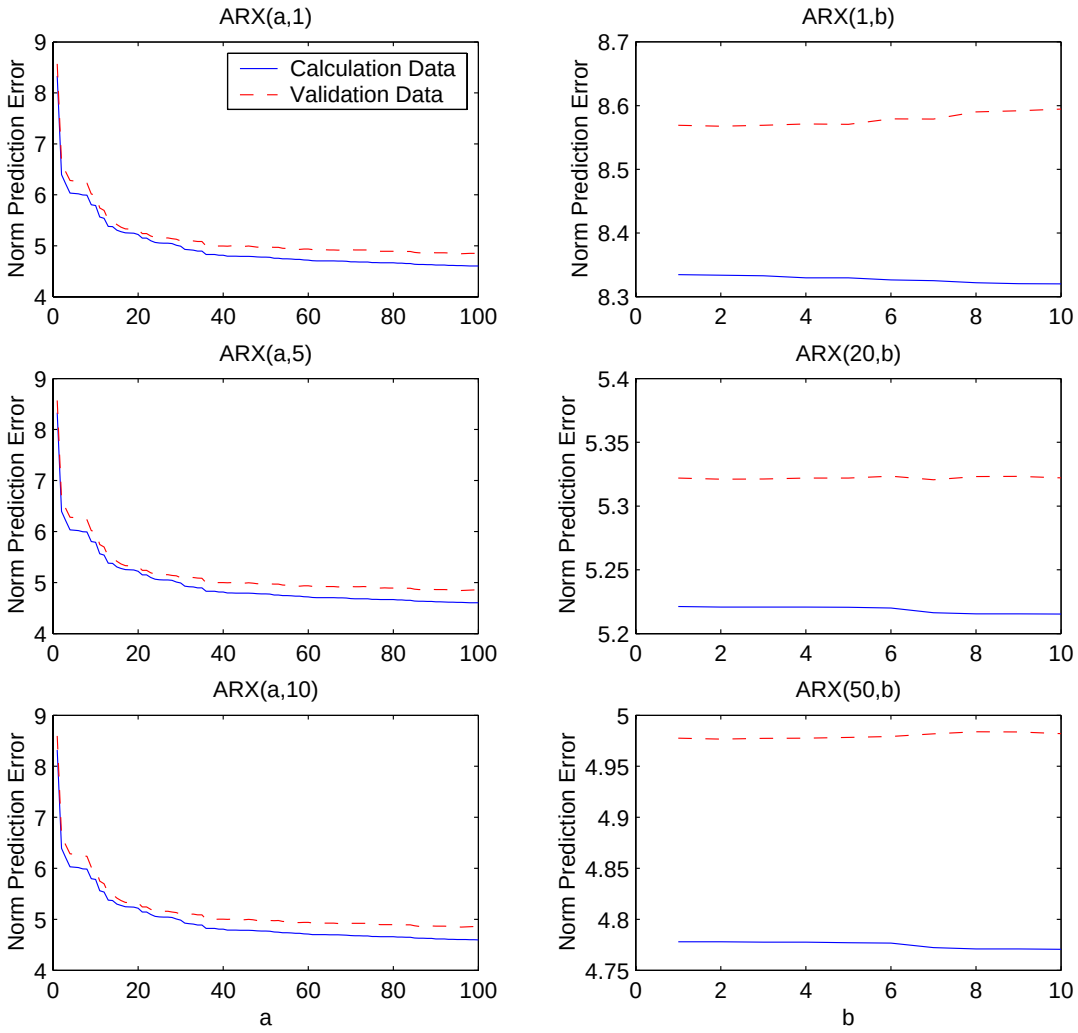

Fig. 8. The ARX prediction error norm for changes in the model order (The calculation data set corresponds to a 0.3V white noise input and the validation data set corresponds to a 0.4V white noise excitation)

$$H(z) = \frac{Y(z)}{U(z)} = \frac{b_1 z^{-1} + \cdots b_{n_{ba}} z^{-n_b}}{1 + a_1 z^{-1} + \cdots a_{n_a} z^{-n_a}} \tag{7}$$

The denominator of the transfer function is the characteristic equation of the dynamic system and encapsulates information on the frequency and damping ratio of each vibration mode of the system. The roots of the characteristic equation are termed the poles of the system and uncouple the orthogonal set of modes. The frequency and damping ratio of the modes can be found from the complex valued pole (where T denotes the time step of the discrete-time signal):

$$z = e^{\left(-\xi\omega_n \pm \omega_n \sqrt{1-\xi^2}\, j\right)T} \tag{8}$$

The migration of the transfer function poles will move as a result of damage; this migration is due to the structural damage influencing the frequency and damping ratios of some of the system vibration modes. To determine the roots of the characteristic equation, numerical algorithms based on Laguerre's formulas are being explored for adoption[17].

5. CONCLUSIONS

Many innovative technologies are being explored for use in structural monitoring systems in order to reduce their installation costs and enhance their functionality. This study has explored the feasibility of including an actuation interface within a self-contained wireless sensing unit. Capable of commanding structural actuators and active sensors, the resulting wireless active sensing unit would be able to enjoy direct interface to the physical system in which it is installed. In particular, active sensors would be a powerful tool to employ in a structural health monitoring system because they can impart low-energy excitations into structural elements that illuminate their high-order response modes. Tracking high-order response modes for the detection of damage is desirable because these modes are sensitive to the onset of damage but are less sensitive to temperature variations than global response modes. Furthermore, screening a structure for damage on an element by element basis preserves the self-sufficiency of the wireless active sensing unit and reduces the amount of wireless communications needed to transfer data thereby saving battery power.

To illustrate the performance of a prototype wireless active sensing unit, an aluminum plate with two piezoelectric pads epoxy mounted to its surface was employed. White noise excitations are applied to the plate by one pad while the unit simultaneously records the response of the second piezoelectric pad. After collection of the system response, software embedded in the computational core was utilized to calculate an ARX time-series model for the input-output measurement data. As part of a larger damage detection methodology that identifies damage from the migration of ARX transfer function poles, the straight-forward but non-trivial ARX software implementation demonstrates the possibility of developing a self-actuated wireless active sensing unit capable of autonomously diagnosing the health of a structures.

ACKNOWLEDGEMENTS

This research is partially funded by the National Science Foundation under grant number CMS-9988909. Additional support has been provided by Los Alamos National Laboratory, Contract Number 75067-001-03.

REFERENCES

1. E. G. Straser and A. S. Kiremidjian. *A modular, wireless damage monitoring system for structures*. Report No. 128, John A. Blume Earthquake Engineering Center, Department of Civil and Environmental Engineering, Stanford University, Stanford, CA, 1998.
2. J. P. Lynch. *Decentralization of wireless monitoring and control technologies for smart civil structures*. Report No. 140, John A. Blume Earthquake Engineering Center, Department of Civil and Environmental Engineering, Stanford University, Stanford, CA, 2002.
3. J. P. Lynch, K. H. Law, A. S. Kiremidjian, E. Carryer, C. R. Farrar, H. Sohn, D. Allen, B. Nadler and J. Wait. "Design and performance validation of a wireless sensing unit for structural monitoring applications", *Structural Engineering and Mechanics*, Techno Press, 17(4), in press, 2004.
4. S. W. Doebling, C. R. Farrar, M. B. Prime and D. W. Shevitz. *Damage identification and health monitoring of structural and mechanical systems from changes in their vibration characteristics: a literature review.* Report No. LA-13070-MS, Los Alamos National Laboratory, Los Alamos, NM, 1996.
5. J. L. Humar, A. Bagchi and H. Xu. "Challenges in vibration-based structural health monitoring." *Proceedings of the 1st International Conference on Structural Health Monitoring and Intelligent Infrastructure*, Balkema Publishers, Tokyo, Japan, pp. 503-511, 2003.
6. G. Park, H. H. Cudney and D. J. Inman, "Impedance-based health monitoring of civil structural components." *Journal of Infrastructure Systems*, ASCE, 6(3): 153-160.
7. R. R. Brooks and S. S. Iyengar. *Multi-sensor fusion*. Prentice Hall, Upper Saddle River, NJ, 1998.
8. S. Bhalla and C. K. Soh. "Structural impedance based damage diagnosis by piezo-transducers," *Earthquake Engineering and Structural Dynamics*, Wiley, 32(12): 1897-1916, 2003.
9. F. Wu and F. K. Chang, "A built-in active sensing diagnostic system for civil infrastructure systems," *Proceedings of 8th International Symposium on Smart Structures and Materials*, San Diego, CA, SPIE v. 4330, pp. 27-35, 2001.
10. Motorola Corp. *Motorola PowerPC MPC555 user's manual*. Motorola Corporation, Phoenix, AZ, 2002.
11. Texas Instruments. *DAC7624: 12-bit quad voltage output digital to analog converter*. Texas Instruments, Inc., Dallas, TX, 1997.
12. MaxStream. *XCite Advanced Programming and Configuration: Advanced Manual*. MaxStream, Inc., Lindon, UT, 2003.

13. J. P. Lynch, A. Sundararajan, K. H. Law, A. S. Kiremidjian and E. Carryer. "Power-efficient data management for a wireless structural monitoring system." *Proceedings of the 4th International Workshop on Structural Health Monitoring*, Stanford, CA, pp. 1177-1184, 2003.
14. Energizer. *L91 AA Battery Data Sheet*. Energizer, Corp., St. Louis, MO, 2001.
15. J. P. Lynch. "Linear Classification of System Poles for Structural Damage Detection using Piezoelectric Active Sensors." *Proceedings of Sensors and Smart Structures Technologies for Civil, Mechanical and Aerospace Systemss,* SPIE, San Diego, CA, 2004.
16. L. Ljung. *System Identification: Theory for the User*. Prentice Hall PTR, Upper Saddle River, NJ, 1999.
17. W. H. Press, S. A. Teukolsky, W. T. Vetterling and B. P. Flannery. *Numerical Recipes in C: The Art of Scientific Computing.* Cambridge University Press, Cambridge, U.K., 1992.